Alone in a crowd: Effect of a nonfunctional lateral line on expression of the social hormone *parathyroid hormone 2*.

Alexandra Venuto[1], Cameron P. Smith[1,2], Marybelle Cameron-Pack[3], and Timothy Erickson[3]

1. East Carolina University, Greenville, NC, USA
2. East Carolina University School of Dental Medicine, Greenville, NC, USA
3. University of New Brunswick, Fredericton, NB, CAN

Corresponding author: Timothy Erickson, timothy.erickson@unb.ca

Key words: hair cells, lateral line, neuropeptide, parathyroid hormone, social brain, zebrafish

SUMMARY STATEMENT

Expression of the pro-social neuropeptide *pth2* is downregulated in larval zebrafish with a congenital loss of lateral line function. Thus, even in social environments, fish with compromised lateral lines may experience chronic loneliness.

ABSTRACT

Parathyroid hormone 2 (Pth2) is a vertebrate-specific neuropeptide whose thalamic expression is upregulated by social contact with conspecifics. However, social interactions fail to stimulate *pth2* expression in isolated zebrafish whose lateral line hair cells have been chemically ablated. These results suggest that modulation of *pth2* by social context is acutely dependent on mechanosensory information from the lateral line. However, it is unclear how a congenital loss of lateral line function influences the ability of zebrafish to interpret their social environment. In this study, we measure *pth2* levels in zebrafish mutants lacking hair cell function in either the lateral line only, or in both the inner ear and lateral line. Socially-raised lateral line mutants express lower levels of *pth2* relative to wild type siblings, but there is no further reduction when all sensory hair cells are nonfunctional. However, social isolation of hair cell mutants causes a further reduction in *pth2* expression, pointing to additional unidentified sensory cues that influence *pth2* production. Lastly, we report that social context modulates fluorescent transgenes driven by the *pth2* promoter. Altogether, these data suggest that lateral line mutants experience a chronic sense of isolation, even when raised in a social environment.

INTRODUCTION

The complex relationship between the brain and social behavior has been studied across animal species for decades (Brothers, 1990; Chen and Hong, 2018; Kravitz and Huber, 2003; Robinson et al., 2008). Different social contexts can evoke a wide range of emotions, from joy and positivity (Burgdorf and Panksepp, 2006; Panksepp and Burgdorf, 2003) to fear and aggression (Amaral, 2002; Neumann et al., 2010) with a high level of plasticity (Chen and Hong, 2018; Kolb and Whishaw, 2003). In situations of social isolation, many animals exhibit anxious behaviors in addition to neurochemical changes in the brain (Amaral, 2002; Mumtaz et al., 2018; Shams et al., 2017; Weiss et al., 2004).

Social behavior is modulated by a suite of neuropeptides (Adkins-Regan, 2009; O'Connell and Hofmann, 2011; Oldfield and Hofmann, 2011; Panksepp et al., 2007; Schoofs et al., 2017). Parathyroid hormone 2 (Pth2, formerly known as tuberoinfundibular peptide of 39 residues or TIP39) is a neuropeptide expressed in the vertebrate thalamus, which is a sensory integration and relay center (Anneser et al., 2020; Bhattacharya et al., 2011; Dobolyi et al., 2012; Mueller, 2012). In rodents, the PTH2 receptor is expressed in several nuclei throughout the central nervous system (Dobolyi et al., 2012). Zebrafish have two *pth2r* paralogs, *pth2ra* and *pth2rb,* each with distinct expression patterns in the fish brain (Seitz, 2019). Activation of PTH2R increases intracellular cAMP levels and can modulate neuroendocrine activity in the hypothalamic–pituitary–adrenal (HPA) axis (Dimitrov and Usdin, 2010). PTH2-PTH2R signaling influences several behaviors, including maternal care (Cservenák et al., 2013), pain sensitivity (Dimitrov et al., 2010; Dimitrov et al., 2013; LaBuda and Usdin, 2004), and anxiety-like responses (Anneser et al., 2022; Coutellier and Usdin, 2011; LaBuda et al., 2004).

Recent work suggests that Pth2 signaling promotes social interactions between conspecifics. In zebrafish, *pth2* mutants exhibit decreased preference for conspecifics (Anneser et al., 2022), while chemogenetic activation of the Pth2-positive region of the rodent brain promotes social contact (Keller et al., 2022). Consistent with this, expression of *pth2* itself positively scales with the quantity of social interactions with conspecifics (Anneser et al., 2020; Anneser et al., 2022; Keller et al., 2022). In rodents, physical touch from conspecifics activates *Pth2* expression (Cservenák et al., 2013; Keller et al., 2022). In addition to tactile touch sensation, fish also have another form of "distant touch" through the mechanosensory lateral line (Dijkgraaf, 1963). The mechanosensory lateral line is a hair cell-based system in aquatic vertebrates that senses hydrodynamic information, such as that created by conspecifics (Butler and Maruska, 2015; Butler and Maruska, 2016a; Butler and Maruska, 2016b; Groneberg et al., 2020; Montgomery et al., 2013). In zebrafish, chemical ablation of the mechanosensory lateral line prevents the rescue of *pth2* expression by a social environment following isolation (Anneser et al., 2020). Therefore, social "touch" (direct contact in rodents and hydrodynamic communication in zebrafish) seems to be a primary sensory activator of *pth2* expression.

Despite this knowledge, there remain several unanswered questions regarding the social regulation of *pth2* expression. First, how do zebrafish interpret social context when they are born without lateral line function? Secondly, do mechanosensory hair cells in the inner ear contribute

to the ability of zebrafish larvae to respond to social context? Thirdly, is *pth2* expression regulated solely via mechanosensation, or can fish use additional sensory inputs to sense the presence of conspecifics? Here, we report that the congenital loss of mechanosensory hair cell function leads to chronically depressed levels of *pth2* expression in socially-housed larval zebrafish. Interestingly, social isolation of hair cell mutants further decreases *pth2* levels, suggesting that larval fish use additional sensory information to sense conspecifics and modulate *pth2* expression. Lastly, we utilize fluorescent reporters driven by the *pth2* regulatory region to evaluate the morphology of *pth2*-expressing cells and visualize *pth2* dynamics *in vivo*. Overall, this study offers additional insight into the sensory basis for social interactions in zebrafish and introduces novel tools to track *pth2* expression in living fish.

RESULTS

Decreased *pth2* expression in larval zebrafish with a genetically disabled lateral line.

pth2 expression decreases when fish are raised in isolation but increases following a brief period of social interaction with conspecifics. However, when the mechanosensory lateral line is ablated in isolated fish prior to social exposure, *pth2* expression levels remain low (Anneser et al., 2020). This implicates the lateral line sensory system in recognizing conspecifics to stimulate *pth2* expression. To further evaluate the role of the lateral line in social recognition, we raised lateral line-deficient mutants (*lhfpl5b*$^{-/-}$) and their siblings in separate social groups and detected *pth2* expression by mRNA *in situ* hybridization (ISH). Socially-raised lateral line mutants exhibit a decrease in *pth2* expression compared to wild type (WT) siblings (Fig. 1B, C), both in terms of a qualitative decrease in the intensity of staining as well as a significant decrease in the number of detectable *pth2*-positive cells (One-tailed Welch's t-test, WT Soc: M = 29.9, SD = 1.7; MUT Soc: M = 9.7, SD = 4.3; $p < 0.0001$) (Fig. 1D). We also ablated lateral line hair cells in socially raised WT larvae using repeated neomycin treatments (Venuto and Erickson, 2021) (Figure 1E). Even though these larvae had social experience prior to losing lateral line input, they exhibited low levels of *pth2* expression similar to lateral line mutants. These results confirm that the loss of lateral line function impairs the ability of *pth2* cells to respond to social context.

103 **Mechanosensory input from inner ear hair cells do not contribute to *pth2* expression.**

104 A low level of *pth2* expression remains in socially-raised lateral line mutants (Fig. 1B, C).
105 To determine if mechanosensory input from the inner ear was responsible for this remaining *pth2*
106 expression, we used three different types of mutations that disable hair cells of both the lateral line
107 and inner ear to compare to the lateral line mutant (*lhfpl5b*$^{-/-}$) and wild type zebrafish. Two of these
108 mutations (*pcdh15a*$^{-/-}$ and *tomt*$^{-/-}$) render the mechano-electrical transduction channel
109 nonfunctional in all hair cells, similar to how the *lhfpl5b* mutation specifically disables lateral line
110 hair cells (Erickson et al., 2017; Erickson et al., 2020; Maeda et al., 2017). The third mutant
111 disables the voltage-gated calcium channel in hair cells (*cacna1da*$^{-/-}$), thereby blocking stimulus-
112 dependent glutamate release (Sheets et al., 2012; Sidi et al., 2004). Again, we measured *pth2*
113 expression via mRNA ISH (Fig. 2B-F) as well as quantitative PCR (qPCR) (Fig. 2G). All hair cell
114 mutants exhibit similarly low levels of *pth2* expression when raised socially, with no additional
115 decrease seen in zebrafish with genetically disabled inner ear and lateral line sensory function
116 (One-way ANOVA with Tukey post-test, $\alpha = 0.05$). From these experiments, we find that inner
117 ear mechanosensory hair cells do not contribute to the regulation of *pth2* expression.
118

119 **Social isolation further reduces *pth2* expression in sensory hair cell mutants.**

120 Chemosensory and visual perception of conspecifics does not significantly rescue *pth2*
121 expression in larval zebrafish raised in isolation (Anneser, et al., 2020). However, since disabling
122 both the lateral line and the inner ear does not completely eliminate *pth2* expression, other non-
123 hair cell-based sensory systems may contribute to the modulation of *pth2* by social context. To test
124 this, we compared *pth2* expression in social and isolated *lhfpl5b* and *tomt* mutants by both mRNA
125 ISH (Fig. 3A-C) and qPCR (Fig. 3D). If *pth2* responds to conspecific signals solely via the lateral
126 line, we expect to see equivalently low expression in mutants raised in social and isolated
127 environments. However, we find this not to be the case. Instead, isolated *lhfpl5b* and *tomt* mutants
128 express less *pth2* than social mutant siblings (One-way ANOVA with Tukey post-test, $\alpha = 0.05$).
129 *pth2* levels in isolated mutants and wild types are indistinguishable. Because social isolation
130 further reduces *pth2* expression in lateral line mutants, we conclude that *pth2* responds to
131 multisensory input during social experience.
132

133 **Morphology of *pth2*-expressing cells using fluorescent reporters.**

134 Fluorescent reporters provide information about the morphology and function of cells,
135 along with the ability to quantify gene expression in living organisms (Choe et al., 2021; Soboleski
136 et al., 2005). Therefore, we created stable lines of transgenic zebrafish expressing GFP or RFP
137 under control of the presumptive *pth2* promoter. These transgenes allow us to visualize the
138 morphology of the *pth2*-expressing cells in living larvae (Fig. 4 and S1). Imaging of transgenic
139 larvae reveals the two bilateral cell clusters with complex projection patterns (Fig. 4B). The
140 anterior ipsilateral projections converge into a dense neuropil in the forebrain, while other fibers
141 project ventrally and posteriorly toward the midbrain. Additionally, we find ventral projections
142 that cross the midline between the two cell clusters. This morphology is consistent in both the GFP
143 and RFP transgenes.

144

145 **The *pth2* transgenes respond to lateral line input and social context.**

146 Next, we tested if the transgene responds to social context (Fig. 5). Consistent with our
147 mRNA ISH and qPCR results, transgenic *lhfpl5b* mutants (Fig. 5A-C) and isolates (Fig. 5D-F)
148 both exhibit a significant decrease in the number of fluorescent cells relative to control siblings
149 (Fig. 5C: One-tailed Welch's t-test, WT Soc: M = 43.2, SD = 3.9; MUT Soc: M = 34.2, SD = 2.8;
150 $p < 0.0001$) (Fig. 5F: One-tailed Welch's t-test, WT Soc: M = 37.3, SD = 2.6; WT Iso: M = 28.3,
151 SD = 2.8; $p < 0.0001$). To gauge whether isolation specifically diminishes expression from the
152 *pth2*-driven transgenes, we compared the effect of social isolation on transgene expression in
153 *Tg(pth2:TagRFP)unb3* and *Tg(slc6a3:EGFP)ot80* larvae. The *slc6a3:*EGFP transgene expresses
154 GFP under control of the dopamine transporter promoter and marks a population of dopaminergic
155 cells in the pretectum, which lies dorsally to the *pth2*-expressing cells. The number of
156 dopaminergic cells in the pretectum do not change in response to social context (One-tailed
157 Welch's t-test, WT Soc: M = 44.0, SD = 4.3; WT Iso: M = 45.1, SD = 4.7; $p = 0.3$) (Fig. 5D-F).
158 These experiments demonstrate that the *pth2* transgenes respond to social context and allows for
159 a wide variety of future experiments to better understand how *pth2* is regulated.

160

161 **DISCUSSION**

162 Previous work revealed that larval zebrafish use lateral line information to sense the
163 presence of conspecifics, leading to upregulation of the social hormone Pth2. Here, we show that

164 *pth2* levels are chronically depressed in socially-raised larvae born without lateral line function.
165 However, social isolation further reduces *pth2* levels in lateral line mutants, suggesting that other
166 socially-derived sensory information can modulate *pth2* expression.
167
168 **The mechanosensory lateral line mediates *pth2* expression.**
169 Anneser, et al. (2020) implicated hydrodynamic stimuli from conspecifics as a key social
170 cue that upregulates production of the neuropeptide Pth2. Isolated larvae with chemically ablated
171 lateral lines fail to upregulate *pth2* when returned to a social environment. In the present study, we
172 use mutant zebrafish with a congenital loss of lateral line function to confirm that hydrodynamic
173 information modulates *pth2* expression. Furthermore, we find that repeated chemical ablation of
174 the lateral line also impairs the ability of social larvae to express *pth2*, even when exposed to
175 conspecifics prior to loss of lateral line function. Our approach complements that of Anneser et al.
176 by providing genetic evidence that *pth2* is modulated by lateral line sensory information (Fig. 1).
177 We conclude that, in terms of Pth2 production, zebrafish born without a lateral line effectively feel
178 alone even when raised in a social context.
179
180 **Auditory and vestibular stimuli do not modulate *pth2* expression in larval zebrafish.**
181 Inner ear hair cells are functionally and structurally similar to lateral line hair cells, and
182 fish use auditory and vestibular sensory information in a variety of behaviors (Bagnall and
183 Schoppik, 2018; Kohashi et al., 2012; Nicolson et al., 1998; Privat et al., 2019). Given that some
184 *pth2* expression remains in lateral line mutants, we examined whether sensory information from
185 the inner ear contributes to social modulation of *pth2.* Using zebrafish with mutations that disable
186 both inner ear and the lateral line hair cells, we find that there is no additional loss of *pth2*
187 expression compared to the lateral line-only mutant (Fig. 2). In addition, we asked if different types
188 of mutations to hair cells impact *pth2* expression. Three of the mutant lines used in this study,
189 *lhfpl5b, tomt* and *pcdh15a,* render the mechanotransduction (MET) channel non-functional
190 (Erickson et al., 2017; Erickson et al., 2020; Maeda et al., 2017), and one mutant line, *cacna1da /*
191 *cav1.3a,* affects the voltage-gated calcium channel (Sheets et al., 2012; Sidi et al., 2004). While
192 both components are necessary for proper hair cell signal transduction, there are key differences
193 between the types of mutations. For mutants affecting the MET channel, potassium and calcium
194 ions are unable to enter the cell in response to stimuli, but the potential for spontaneous calcium

influx and neurotransmitter release remains (Trapani and Nicolson, 2011). Whereas for the calcium channel mutation, ions enter through the MET channel but there is no evoked or spontaneous neurotransmitter release. Regardless, all mutations that disrupt hair cell function result in the same decrease of *pth2* expression in socially raised fish compared to their wild type siblings (Fig. 2). Therefore, we conclude that regulation of *pth2* by social context is primarily via the mechanosensory lateral line in larval zebrafish and that auditory and vestibular information does not contribute.

Additional socially-derived sensory cues modulate *pth2* expression.

Anneser et al. (2020) demonstrated that neither chemical nor visual cues from conspecifics significantly restored *pth2* expression in isolated larvae. In our study, we found that isolation further reduced *pth2* expression in lateral line mutants to the same level as isolated wild types (Fig. 3). This indicates that additional sensory modalities contribute to the regulation of *pth2* expression. It will be informative to test whether the photo- or chemosensory systems can modulate *pth2* expression under sensitized circumstances in which hydrosensory information is compromised. Additionally, it is possible that tactile stimuli are contributing to *pth2* regulation in zebrafish, consistent with the effects of social touch in rodents. Future work is necessary to test this theory.

Visualizing *pth2* expression *in vivo.*

We used *pth2* promoter-driven fluorescent transgenes to visualize *pth2*-expressing cells and their projections. Consistent with the Anneser, et al. (2020) whole-mount immunostains, we see Pth2-positive cells located in bilateral clusters in the thalamus that feature lateral neurites, anterior ipsilateral projections terminating as a loosely organized neuropil in the telencephalon, as well as posterior ipsilateral projections. The transgene reveals additional fibers that project ventrally from the cell bodies and cross the midline, potentially contacting the contralateral *pth2*-expressing cluster (Fig. 4 and Supplemental Movie 1). Investigating the morphology of these cells will help us understand the cellular targets of Pth2 signaling and how activity of the two clusters is coordinated.

We also tested the *pth2:EGFP* and *pth2:TagRFP* transgenic lines as a proxy for *pth2* expression *in vivo* and found that both lateral line mutants and isolated wild type larvae exhibit fewer GFP/RFP-positive cells than socially raised siblings (Fig. 5). In contrast, the number of

226 dopaminergic cells located dorsally to the *pth2* clusters exhibited no change to social context.
227 Dopamine has been implicated in sensation and social interaction (Haehnel-Taguchi et al., 2018;
228 Saif et al., 2013; Shams et al., 2018), and our results indicate that the social modulation of *pth2* is
229 distinct from the dopaminergic system in this brain region in larval zebrafish. While our results
230 with the *pth2* transgenes agree with our *in situ* hybridization and qPCR results (Fig. 1, 3), we note
231 that the effects of isolation and lateral line deficiency on transgene expression are not as
232 pronounced as when assaying for endogenous *pth2* mRNA and protein. It could be that the post-
233 transcriptional and / or post-translation regulation of fluorescent proteins do not reflect regulation
234 of endogenous *pth2* transcription and protein stability. It is also possible that the *pth2* promoter
235 region we use to drive the transgene is missing some critical regulatory elements. Future work will
236 strive to distinguish between these possibilities and to optimize the transgene for capturing *pth2*
237 properties in vivo.
238 Overall, our results confirm that *pth2* expression is modulated by the mechanosensory
239 lateral line (Fig. 1). We also show that the lateral line is the only hair-cell based sensory organ
240 regulating *pth2* expression (Fig. 2). However, due to expression levels being slightly higher in
241 social lateral line mutants compared to the same mutants or wild type larvae raised in isolation, we
242 conclude that there must be unidentified sensory system(s) that contribute to the modulation of
243 *pth2* (Fig. 3). Finally, we created transgenic lines to visualize the morphology of *pth2*+ cells *in*
244 *vivo* (Fig. 4), and report that the transgenes respond to social context (Fig. 5). These transgenic
245 lines can be used in future studies to elucidate the role of *pth2* in zebrafish. Taken together, this
246 work suggests that zebrafish without a functioning lateral line experience a chronic sense of
247 isolation, even in a social context.
248
249 **MATERIALS AND METHODS**
250 **Ethics statement**
251 Animal research complied with guidelines stipulated by the Institutional Animal Care and
252 Use Committees at East Carolina University (Greenville, NC, United States) and at University of
253 New Brunswick (Fredericton, New Brunswick, Canada). Zebrafish (*Danio rerio*) were maintained
254 and bred using standard procedures (Westerfield, 2000). All experiments used larvae at 1–5 days
255 post-fertilization (dpf), which are of indeterminate sex at this stage.
256

257 **Mutant and transgenic fish lines**

258 The following previously described zebrafish mutant and transgenic lines were used in this
259 study: *lhfpl5b*^{vo35}, *pcdh15a*^{th263b}, *tomt*^{tk256c}, *cacna1da*^{tc323d}, and *Tg(slc6a3:EGFP)ot80* (Erickson et
260 al., 2017; Erickson et al., 2020; Maeda et al., 2017; Sidi et al., 2004; Xi et al., 2011). To make the
261 *Tg(pth2:EGFP)unb2* and *Tg*(*pth2:TagRFP)unb3* transgenic lines, 2067 base pairs immediately
262 upstream of the *pth2* coding region (including the 5' UTR and first intron) were PCR amplified
263 with primers containing attB4-B1 recombination sites (*pth2*-specific sequence underlined: Fwd:
264 GGGGACAACTTTGTATAGAAAAGTTGGTAAAGGACACTCTTTGAGATCCT, Rvs:
265 GGGGACTGCTTTTTTGTACAAACTTGCCTGCAGATGAATAAGTTGAATAATACA. The
266 PCR product was cloned into the Gateway pDONR-P4-P1R entry vector by a standard BP clonase
267 reaction and an Multisite LR reaction was performed to create *pth2:EGFP-pA, cryaa:EGFP* and
268 *pth2:tagRFP-pA, cryaa:mCherry* plasmids. pDestTol2pACryGFP and pDESTtol2pACrymCherry
269 plasmids were gifts from Joachim Berger & Peter Currie (Addgene plasmids # 64022, 64023). The
270 expression constructs were co-injected with *tol2* transposase mRNA into 1-cell zebrafish embryos
271 (Kwan et al., 2007). F0 founders were outcrossed to produce stable F1 transgenics. At a minimum,
272 progeny from F2 transgenics were used in this study.

273

274 **Social isolation experiments for *in situ* hybridization, qPCR, and transgenic lines**

275 Zebrafish larvae were sorted for *lhfpl5b*^{vo35}, *pcdh15a*^{th263b}, *tomt*^{tk256c} homozygotes at 2 dpf
276 with FM1-43 dye labelling. *cacna1da*^{tc323d} homozygotes were identified behaviorally at 4 dpf.
277 *Tg*(*pth2:EGFP)* and *Tg*(*pth2:TagRFP)* transgenics were identified by their GFP or mCherry lens
278 markers, respectively. *Tg(slc6a3:EGFP)*-positive larvae were identified by GFP expression in the
279 brain. Identified larvae were divided into social groups of thirty larvae, while another thirty larvae
280 were placed in isolation. Both social and isolated larvae were housed in 6-well tissue culture plates
281 containing 5 ml of E3 embryo media. Strips of paper were placed between each well to prevent
282 visual access between wells. Larvae intended for mRNA *in situ* hybridization (ISH) were grown
283 in E3 with 200 µM N-Phenylthiourea (PTU) (Alfa Aesar) to prevent pigment formation. Each
284 group was incubated at 28.5ºC with a 14L:10D photoperiod from 2 to 4 dpf. At 4 dpf, larvae were
285 either fixed for *in situ* hybridization, processed for qPCR, or imaged to visualize the transgene.

286

287

288 **Repeated neomycin treatments**

289 The repeated neomycin treatments were performed essentially as previously described
290 (Venuto & Erickson, 2021). At 24 hpf, WT embryos were divided into two groups of 30 and
291 grown continuously in media supplemented with 200 µM PTU to prevent pigment formation.
292 Larvae were manually dechorionated at 2 dpf. Starting at 9:00 AM, 3 dpf larvae were exposed to
293 either 0 or 50 µM neomycin sulfate hydrate (Alfa Aesar) for 30 minutes at 28ºC every 12 hours.
294 At noon on 4 dpf, treated and untreated groups of larvae were anesthetized with 0.016% MS-222
295 and fixed in 4% PFA for mRNA ISH. The experiment was repeated twice using 30 larvae per
296 treatment group.

297

298 **mRNA in situ hybridization**

299 The *pth2* in situ probe sequence was amplified using the Invitrogen SuperScript IV One-
300 Step RT-PCR kit (ThermoFisher) using the following forward and reverse primers: F:
301 CATTGCATGGACGATTTACG; R: TGCCATGTCATTCAAAATCC. The RT-PCR product
302 was purified by gel extraction and propagated in the pCR4-TOPO vector. The pCR4-*pth2* plasmid
303 was linearized with NotI and the antisense DIG-labeled ISH probe was made using the T3 RNA
304 polymerase promoter. Probe synthesis and in situ hybridization were performed essentially as
305 described (Erickson et al., 2010). Larvae were imaged at 20X magnification using an Olympus
306 BH-2 microscope outfitted with a Jenoptik Gryphax Arktur camera.

307

308 **RNA isolation and real time quantitative PCR (qPCR)**

309 For RNA isolation, 10 whole larval heads were used per replicate. Samples were collected
310 on ice, placed in 1.7 mL RNase-free microcentrifuge tubes containing 200 µl RNAzol (Molecular
311 Research Center, Inc., OH. Catalog: RN 190) and homogenized immediately. Total RNA was
312 extracted from homogenized solutions according to the manufacturer's protocol. For each sample,
313 cDNAs was synthesized using 1 µg total RNA and a high-capacity cDNA Reverse Transcription
314 kit (Thermo Fisher Scientific, Waltham, Massachusetts, USA, Catalog#4368814) following the
315 manufacturer's instructions.

316 The levels of *pth2* transcripts were determined by quantitative real-time PCR (qPCR) using
317 SYBR green dye (Invitrogen) and a CFX Connect real-time thermal cycler (Bio-Rad Laboratories,
318 Hercules, California, USA). The qPCR reaction was conducted with initial denaturation at 95 °C

319 for 2 min, followed by 30 cycles of 30 s denaturation at 95 °C, 30 s annealing at 57 °C, and 30 s
320 extension at 72 °C using the specific primers (Forward: CCACGCAACACACAGTCAAG,
321 Reverse: GCAAGTTACTTTGCAGAGGTC) and GoTaq G2 DNA polymerase (Promega,
322 Madison, Wisconsin, USA). Each PCR mixture (15 µl) consisted of 7.795 µl DNase free water,
323 3 µl 5XGoTaq buffer, 1.5 µl 25 mM MgCl2, 0.3 µl 10 mM dNTP mix, 0.15 ml 10µM forward or
324 reverse primer, 2 µl cDNA, 0.03 µl 100X SYBR green dye (final concentration 0.2X), and 0.075
325 µl Taq. The absolute values (copies/µg total RNA) were determined using Ct values of samples
326 and a standard curve generated from serial known concentrations of plasmid containing the target
327 region of *pth2*. The relative expression was computed by calculating the fold change compared to
328 the mean value of the mutant isolated condition. The efficiency of the PCR and authentic PCR
329 products was further confirmed by analyses of melting curve and gel electrophoresis.
330
331 **Transgenic imaging and quantification**
332 Live zebrafish larvae were anesthetized with E3 plus 0.016% MS-222 and mounted
333 dorsally on a depression slide in 1.2% low melting point agarose in E3. EGFP was imaged using
334 a Zeiss LSM800 laser-scanning confocal with a 40x water objective and Zeiss Zen software. To
335 quantify results, cell counts were performed using Fiji/ImageJ image processing software
336 (Schindelin et al., 2012). Depth encoded 2D and 3D projections were created in Fiji/ImageJ using
337 the *Z-stack Depth Color Code 0.0.2* plugin. Figures were assembled in Adobe Photoshop and
338 equally adjusted for brightness and contrast among corresponding treatment groups.
339
340 **Statistical tests**
341 All graphs and statistical tests were done using R (R Core Team, 2021). For *in* situ
342 hybridization cell counts, a one-tailed Welch's t-test was used (two replicates, n = 7-9 larvae per
343 condition per replicate). For the qPCR experiment, a one-way ANOVA with a Tukey post-hoc test
344 was conducted (three replicates, n = 10 per condition per replicate). For the transgenic cell counts,
345 a one-tailed Welch's t-test was used (three replicates, n = 5 per condition per replicate). A p-value
346 of less than 0.05 was considered significant. One-way ANOVAs were used to compare the whole
347 experimental condition (genotype plus social context) as single independent variables. One-tailed
348 t-tests were used due to only having an expectation for a decrease in *pth2* expression following
349 isolation or loss of lateral line sensory information. Sample sizes were determined by the number

of fish used in the experiment. Replicates indicate how many times the experiment was conducted. No samples were excluded from the analysis.

ACKNOWLEDGMENTS

The authors would like to thank Dr. Yong Zhu for providing his reagents and assistance with qPCR experiments, and Dr. Bryan Crawford for helpful comments on the manuscript. We also thank members of the Erickson and Issa labs for their assistance with zebrafish husbandry.

COMPETING INTERESTS

The authors declare no competing interests.

FUNDING

This work was funded by East Carolina University's Division of Research, Economic Development and Engagement (REDE) and The Natural Science and Engineering Research Council (NSERC) of Canada Discovery Grant RGPIN-2021-03166 to T.E.

DATA AVAILABILITY

The datasets generated for this study are available on request to the corresponding author.

REFERENCES

Adkins-Regan, E. (2009). Neuroendocrinology of social behavior. *ILAR Journal* **50**, 5–14.

Amaral, D. G. (2002). The primate amygdala and the neurobiology of social behavior: implications for understanding social anxiety. *Biological Psychiatry* **51**, 11–17.

Anneser, L., Alcantara, I. C., Gemmer, A., Mirkes, K., Ryu, S. and Schuman, E. M. (2020). The neuropeptide Pth2 dynamically senses others via mechanosensation. *Nature 2020 588:7839* **588**, 653–657.

Anneser, L., Gemmer, A., Eilers, T., Alcantara, I. C., Loos, A.-Y., Ryu, S. and Schuman, E. M. (2022). The neuropeptide Pth2 modulates social behavior and anxiety in zebrafish. *iScience* **25**, 103868.

Bagnall, M. W. and Schoppik, D. (2018). Development of vestibular behaviors in zebrafish. *Curr Opin Neurobiol* **53**, 83.

381 **Bhattacharya, P., Yan, Y. L., Postlethwait, J. and Rubin, D. A.** (2011). Evolution of the
382 vertebrate pth2 (TIP39) gene family and the regulation of PTH type 2 receptor (pth2r) and
383 its endogenous ligand pth2 by hedgehog signaling in zebrafish development. *Journal of*
384 *Endocrinology* **211**, 187–200.
385 **Brothers, L.** (1990). The neural basis of primate social communication. *Motivation and Emotion*
386 *1990 14:2* **14**, 81–91.
387 **Burgdorf, J. and Panksepp, J.** (2006). The neurobiology of positive emotions. *Neuroscience &*
388 *Biobehavioral Reviews* **30**, 173–187.
389 **Butler, J. M. and Maruska, K. P.** (2015). The mechanosensory lateral line is used to assess
390 opponents and mediate aggressive behaviors during territorial interactions in an African
391 cichlid fish. *J Exp Biol* **218**, 3284–94.
392 **Butler, J. M. and Maruska, K. P.** (2016a). The Mechanosensory Lateral Line System Mediates
393 Activation of Socially-Relevant Brain Regions during Territorial Interactions. *Frontiers in*
394 *Behavioral Neuroscience* **10**, 93.
395 **Butler, J. M. and Maruska, K. P.** (2016b). Mechanosensory signaling as a potential mode of
396 communication during social interactions in fishes. *The Journal of Experimental Biology*
397 **219**, 2781–2789.
398 **Chen, P. and Hong, W.** (2018). Neural Circuit Mechanisms of Social Behavior. *Neuron* **98**, 16–
399 30.
400 **Choe, C. P., Choi, S.-Y., Kee, Y., Kim, M. J., Kim, S.-H., Lee, Y., Park, H.-C. and Ro, H.**
401 (2021). Transgenic fluorescent zebrafish lines that have revolutionized biomedical research.
402 *Laboratory Animal Research 2021 37:1* **37**, 1–29.
403 **Coutellier, L. and Usdin, T. B.** (2011). Enhanced long-term fear memory and increased anxiety
404 and depression-like behavior after exposure to an aversive event in mice lacking TIP39
405 signaling. *Behavioural Brain Research* **222**, 265–269.
406 **Cservenák, M., Szabó, É. R., Bodnár, I., Lékó, A., Palkovits, M., Nagy, G. M., Usdin, T. B.**
407 **and Dobolyi, A.** (2013). Thalamic neuropeptide mediating the effects of nursing on
408 lactation and maternal motivation. *Psychoneuroendocrinology* **38**, 3070–3084.
409 **Dijkgraaf, S.** (1963). The functioning and significance of the lateral-line organs. *Biological*
410 *Reviews* **38**, 51–105.

411 **Dimitrov, E. and Usdin, T. B.** (2010). Tuberoinfundibular peptide of 39 residues modulates the
412 mouse hypothalamic-pituitary-adrenal axis via paraventricular glutamatergic neurons. *J*
413 *Comp Neurol* **518**, 4375–4394.
414 **Dimitrov, E. L., Petrus, E. and Usdin, T. B.** (2010). Tuberoinfundibular peptide of 39 residues
415 (TIP39) signaling modulates acute and tonic nociception. *Experimental Neurology* **226**, 68–
416 83.
417 **Dimitrov, E. L., Kuo, J., Kohno, K. and Usdin, T. B.** (2013). Neuropathic and inflammatory
418 pain are modulated by tuberoinfundibular peptide of 39 residues. *Proceedings of the*
419 *National Academy of Sciences* **110**, 13156–13161.
420 **Dobolyi, A., Dimitrov, E., Palkovits, M. and Usdin, T. B.** (2012). The Neuroendocrine
421 Functions of the Parathyroid Hormone 2 Receptor. *Frontiers in Endocrinology* **3**, 121.
422 **Erickson, T., French, C. R. and Waskiewicz, A. J.** (2010). Meis1 specifies positional
423 information in the retina and tectum to organize the zebrafish visual system. *Neural*
424 *Development* **5**, 22.
425 **Erickson, T., Morgan, C. P., Olt, J., Hardy, K., Busch-Nentwich, E., Maeda, R., Clemens,**
426 **R., Krey, J. F., Nechiporuk, A., Barr-Gillespie, P. G., et al.** (2017). Integration of
427 Tmc1/2 into the mechanotransduction complex in zebrafish hair cells is regulated by
428 Transmembrane O-methyltransferase (Tomt). *Elife* **6**,.
429 **Erickson, T., Pacentine, I. v., Venuto, A., Clemens, R. and Nicolson, T.** (2020). The lhfpl5
430 Ohnologs lhfpl5a and lhfpl5b Are Required for Mechanotransduction in Distinct
431 Populations of Sensory Hair Cells in Zebrafish. *Frontiers in Molecular Neuroscience* **12**,
432 320.
433 **Groneberg, A. H., Marques, J. C., Martins, A. L., Diez del Corral, R., de Polavieja, G. G.**
434 **and Orger, M. B.** (2020). Early-Life Social Experience Shapes Social Avoidance
435 Reactions in Larval Zebrafish. *Current Biology* **30**, 4009-4021.e4.
436 **Haehnel-Taguchi, M., Fernandes, A. M., Böhler, M., Schmitt, I., Tittel, L. and Driever, W.**
437 (2018). Projections of the diencephalospinal dopaminergic system to peripheral sense
438 organs in larval zebrafish (Danio rerio). *Frontiers in Neuroanatomy* **12**, 20.
439 **Keller, D., Láng, T., Cservenák, M., Puska, G., Barna, J., Csillag, V., Farkas, I., Zelena, D.,**
440 **Dóra, F., Barteczko, L., et al.** (2022). A thalamo-preoptic pathway promoting social touch.
441 *bioRxiv* 2022.01.11.475648.

442 **Kohashi, T., Nakata, N. and Oda, Y.** (2012). Effective Sensory Modality Activating an Escape
443 Triggering Neuron Switches during Early Development in Zebrafish. *The Journal of*
444 *Neuroscience* **32**, 5810.
445 **Kolb, B. and Whishaw, I. Q.** (2003). Brain Plasticity and Behavior.
446 *http://dx.doi.org/10.1146/annurev.psych.49.1.43* **49**, 43–64.
447 **Kravitz, E. A. and Huber, R.** (2003). Aggression in invertebrates. *Current Opinion in*
448 *Neurobiology* **13**, 736–743.
449 **Kwan, K. M., Fujimoto, E., Grabher, C., Mangum, B. D., Hardy, M. E., Campbell, D. S.,**
450 **Parant, J. M., Yost, H. J., Kanki, J. P. and Chien, C.-B.** (2007). The Tol2kit: a multisite
451 gateway-based construction kit for Tol2 transposon transgenesis constructs. *Dev Dyn* **236**,
452 3088–99.
453 **LaBuda, C. J. and Usdin, T. B.** (2004). Tuberoinfundibular peptide of 39 residues decreases
454 pain-related affective behavior. *NeuroReport* **15**, 1779–1782.
455 **LaBuda, C. J., Dobolyi, A. and Usdin, T. B.** (2004). Tuberoinfundibular peptide of 39 residues
456 produces anxiolytic and antidepressant actions. *Neuroreport* **15**, 881–885.
457 **Maeda, R., Pacentine, I. v., Erickson, T. and Nicolson, T.** (2017). Functional Analysis of the
458 Transmembrane and Cytoplasmic Domains of Pcdh15a in Zebrafish Hair Cells. *The Journal*
459 *of Neuroscience* **37**, 3231–3245.
460 **Montgomery, J., Bleckmann, H. and Coombs, S.** (2013). Sensory Ecology and Neuroethology
461 of the Lateral Line. 121–150.
462 **Mueller, T.** (2012). What is the Thalamus in Zebrafish? *Frontiers in Neuroscience* **6**, 64.
463 **Mumtaz, F., Khan, M. I., Zubair, M. and Dehpour, A. R.** (2018). Neurobiology and
464 consequences of social isolation stress in animal model—A comprehensive review.
465 *Biomedicine & Pharmacotherapy* **105**, 1205–1222.
466 **Neumann, I. D., Veenema, A. H. and Beiderbeck, D. I.** (2010). Aggression and anxiety: Social
467 context and neurobiological links. *Frontiers in Behavioral Neuroscience* **4**, 12.
468 **Nicolson, T., Rüsch, A., Friedrich, R. W., Granato, M., Ruppersberg, J. P. and Nüsslein-**
469 **Volhard, C.** (1998). Genetic Analysis of Vertebrate Sensory Hair Cell Mechanosensation:
470 the Zebrafish Circler Mutants. *Neuron* **20**, 271–283.

O'Connell, L. A. and Hofmann, H. A. (2011). Genes, hormones, and circuits: An integrative approach to study the evolution of social behavior. *Frontiers in Neuroendocrinology* **32**, 320–335.

Oldfield, R. G. and Hofmann, H. A. (2011). Neuropeptide regulation of social behavior in a monogamous cichlid fish. *Physiology & Behavior* **102**, 296–303.

Panksepp, J. and Burgdorf, J. (2003). "Laughing" rats and the evolutionary antecedents of human joy? *Physiology & Behavior* **79**, 533–547.

Panksepp, J., Burgdorf, J., Beinfeld, M. C., Kroes, R. A. and Moskal, J. R. (2007). Brain Regional Neuropeptide Changes Resulting From Social Defeat. *Behavioral Neuroscience* **121**, 1364–1371.

Privat, M., Romano, S. A., Pietri, T., Jouary, A., Boulanger-Weill, J., Elbaz, N., Duchemin, A., Soares, D. and Sumbre, G. (2019). Sensorimotor Transformations in the Zebrafish Auditory System. *Current Biology* **29**, 4010-4023.e4.

R Core Team (2021). R: A Language and Environment for Statistical Computing.

Robinson, G. E., Fernald, R. D. and Clayton, D. F. (2008). Genes and social behavior. *Science* **322**, 896–900.

Saif, M., Chatterjee, D., Buske, C. and Gerlai, R. (2013). Sight of conspecific images induces changes in neurochemistry in zebrafish. *Behavioural Brain Research* **243**, 294–299.

Schindelin, J., Arganda-Carreras, I., Frise, E., Kaynig, V., Longair, M., Pietzsch, T., Preibisch, S., Rueden, C., Saalfeld, S., Schmid, B., et al. (2012). Fiji: an open-source platform for biological-image analysis. *Nature Methods 2012 9:7* **9**, 676–682.

Schoofs, L., de Loof, A. and van Hiel, M. B. (2017). Neuropeptides as Regulators of Behavior in Insects. *http://dx.doi.org/10.1146/annurev-ento-031616-035500* **62**, 35–52.

Seitz, N. (2019). Characterization Of Pth Type-2 Receptor (pth2rb) And Its Endogenous Ligand Pth2 in Zebrafish Development. *Theses and Dissertations* 1131. https://ir.library.illinoisstate.edu/etd/1131.

Shams, S., Seguin, D., Facciol, A., Chatterjee, D. and Gerlai, R. (2017). Effect of social isolation on anxiety-related behaviors, cortisol, and monoamines in adult zebrafish. *Behavioral Neuroscience* **131**, 492–504.

500 **Shams, S., Amlani, S., Buske, C., Chatterjee, D. and Gerlai, R.** (2018). Developmental social
501 isolation affects adult behavior, social interaction, and dopamine metabolite levels in
502 zebrafish. *Developmental Psychobiology* **60**, 43–56.
503 **Sheets, L., Kindt, K. S. and Nicolson, T.** (2012). Presynaptic CaV1.3 Channels Regulate
504 Synaptic Ribbon Size and Are Required for Synaptic Maintenance in Sensory Hair Cells.
505 *The Journal of Neuroscience* **32**, 17273.
506 **Sidi, S., Busch-Nentwich, E., Friedrich, R., Schoenberger, U. and Nicolson, T.** (2004).
507 gemini Encodes a Zebrafish L-Type Calcium Channel That Localizes at Sensory Hair Cell
508 Ribbon Synapses. *The Journal of Neuroscience* **24**, 4213.
509 **Soboleski, M. R., Oaks, J. and Halford, W. P.** (2005). Green fluorescent protein is a
510 quantitative reporter of gene expression in individual eukaryotic cells. *The FASEB journal :*
511 *official publication of the Federation of American Societies for Experimental Biology* **19**,
512 440.
513 **Trapani, J. G. and Nicolson, T.** (2011). Mechanism of Spontaneous Activity in Afferent
514 Neurons of the Zebrafish Lateral-Line Organ. *The Journal of Neuroscience* **31**, 1614.
515 **Venuto, A. and Erickson, T.** (2021). Evaluating the Death and Recovery of Lateral Line Hair
516 Cells Following Repeated Neomycin Treatments. *Life* **11**, 1180.
517 **Weiss, I. C., Pryce, C. R., Jongen-Rêlo, A. L., Nanz-Bahr, N. I. and Feldon, J.** (2004). Effect
518 of social isolation on stress-related behavioural and neuroendocrine state in the rat.
519 *Behavioural Brain Research* **152**, 279–295.
520 **Xi, Y., Yu, M., Godoy, R., Hatch, G., Poitras, L. and Ekker, M.** (2011). Transgenic zebrafish
521 expressing green fluorescent protein in dopaminergic neurons of the ventral diencephalon.
522 *Developmental Dynamics* **240**, 2539–2547.
523
524

525 **FIGURES AND LEGENDS:**

526

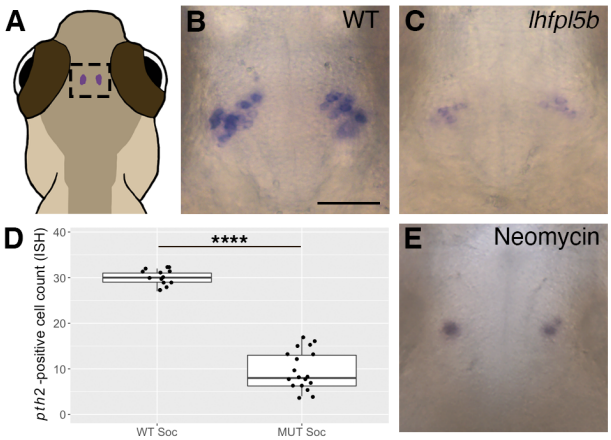

527

528 **Figure 1: Decreased *pth2* expression in lateral line-deficient larval zebrafish.** A: Location of
529 *pth2*-expressing cells in the thalamus. B-C: Representative images of mRNA *in situ* hybridizations
530 (ISH) showing *pth2*-positive cells in socially-reared B) wild type and C) lateral line mutant
531 (*lhfpl5b*^{vo35}) zebrafish at 4 dpf. D) Boxplots of *pth2*-positive cell counts from ISH images (WT =
532 14, MUT = 18 larvae from two replicates). E) Representative mRNA ISH image showing reduced
533 *pth2* expression in a socially-reared larva at 4 dpf whose lateral line was ablated with repeated
534 neomycin treatments. Scale bar is 50 µm and applies to all images. A one-tailed Welch's t-test was
535 used to assess significance, **** = $p < 0.0001$.

536

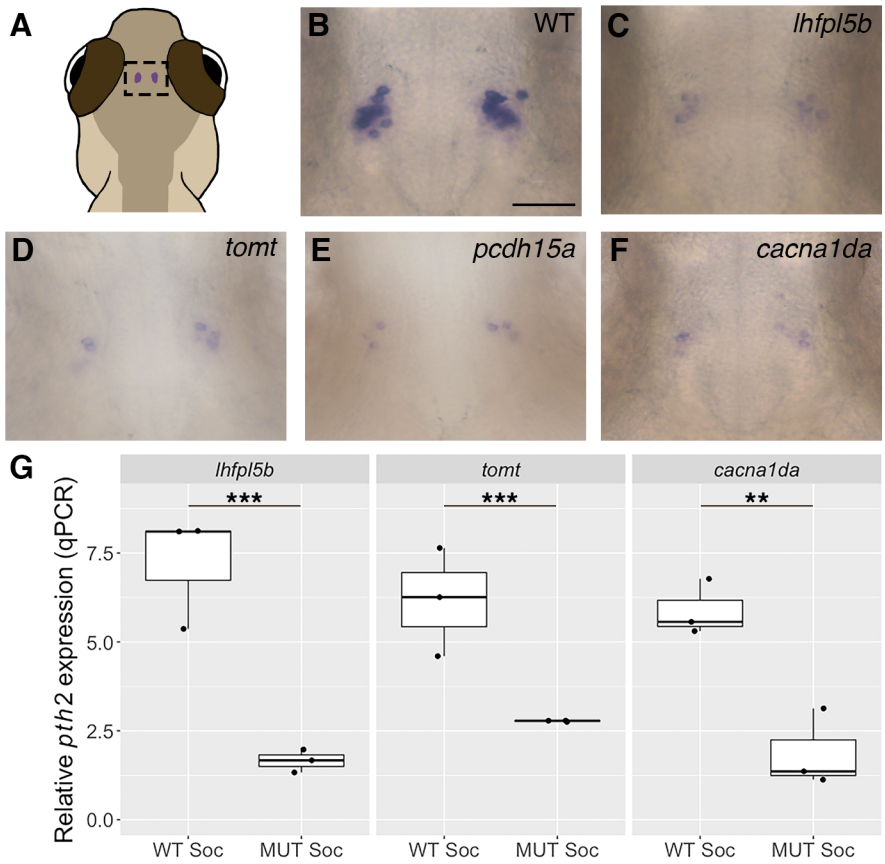

Figure 2: Mechanosensory input from inner ear hair cells does not contribute to *pth2* expression. A: Location of *pth2*-expressing cells in the thalamus. B-F: Representative images of mRNA *in situ* hybridizations (ISH) showing *pth2*-positive cells in socially-reared B) wild type, C) *lhfpl5b*^{vo35}, D) *tomt*^{tk256c}, E) *pcdh15a*^{th263b}, and F) *cacna1da*^{tc323d} larvae at 4 dpf. Scale bar = 50 µm, applies to all images. G: Boxplots of qPCR results showing *pth2* expression in socially-reared mutants and siblings. Three replicates per condition, n = 10 larvae per condition per replicate. One way ANOVA with Tukey post-test to assess significance, *** = $p < 0.001$, ** = $p < 0.01$.

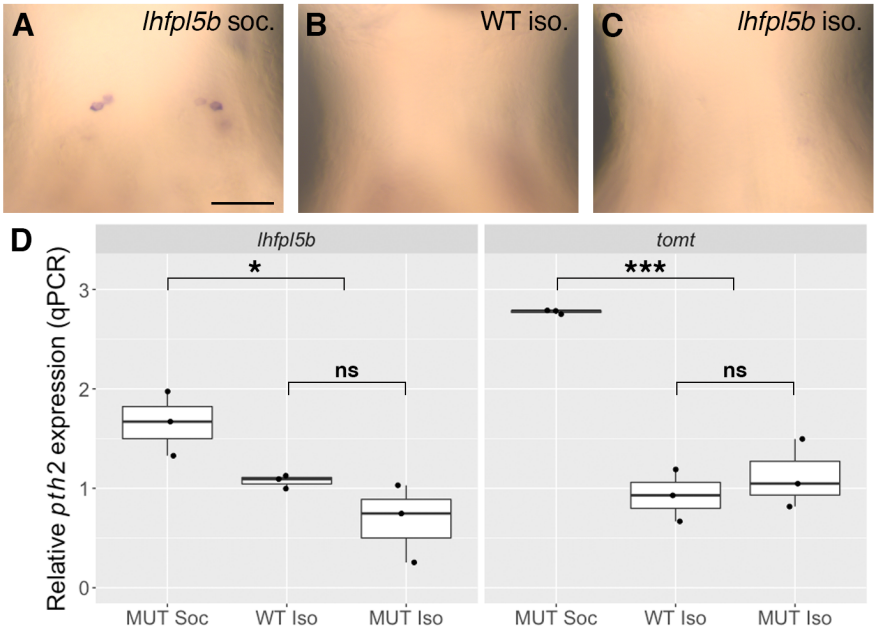

Figure 3: Social isolation further reduces *pth2* expression in sensory hair cell mutants. A-C: mRNA *in situ* hybridization showing representative examples of *pth2*-positive cells in A) socially-reared *lhfpl5b*^{vo35} mutants, B) isolated wild type larvae, and C) isolated *lhfpl5b*^{vo35} mutants. Scale bar = 50 µm, applies to all images. D: Boxplots of qPCR results comparing *pth2* expression in socially-reared *lhfpl5b*^{vo35} and *tomt*^{tk256c} mutants relative to isolated mutant and wild type siblings. Three replicates per condition, n = 10 larvae per condition per replicate. One way ANOVA with Tukey post-test to assess significance, *** = $p < 0.001$, * = $p < 0.05$, ns = not significant.

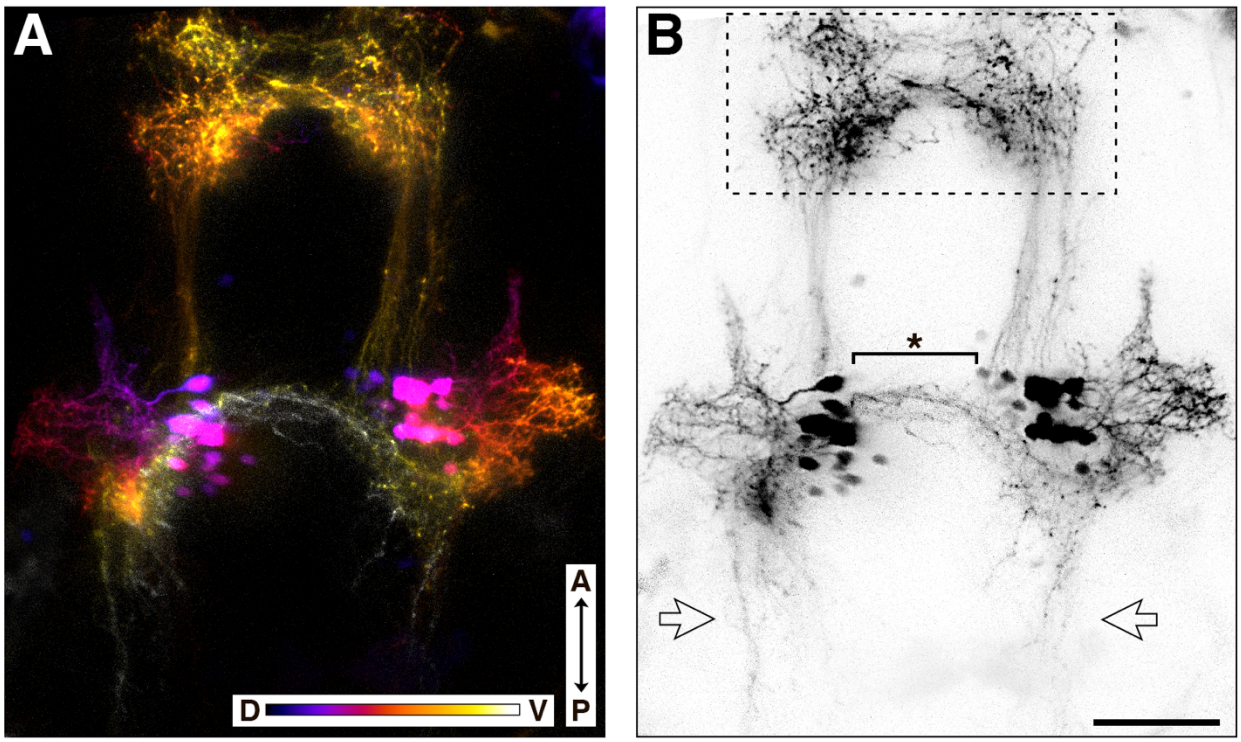

Figure 4: Morphology of *pth2*-expressing cells. A: Representative depth-encoded image of the *Tg(pth2:TagRFP)unb3* transgenic line at 4 dpf. The anterior-posterior (A-P) axis and dorsal-ventral (D-V) depth color scale are indicated at the bottom. B: Black and white version of the image in A. From the top: the dashed box indicates the anterior neuropil, the starred bracket highlights the ventral neurites that cross the midline, and the bilateral open arrows point to posterior neurites. Scale bar in B is 50 µm, applies to both images. See Supplemental Movie 1 for a 3D rendering of the depth-encoded *pth2* transgene.

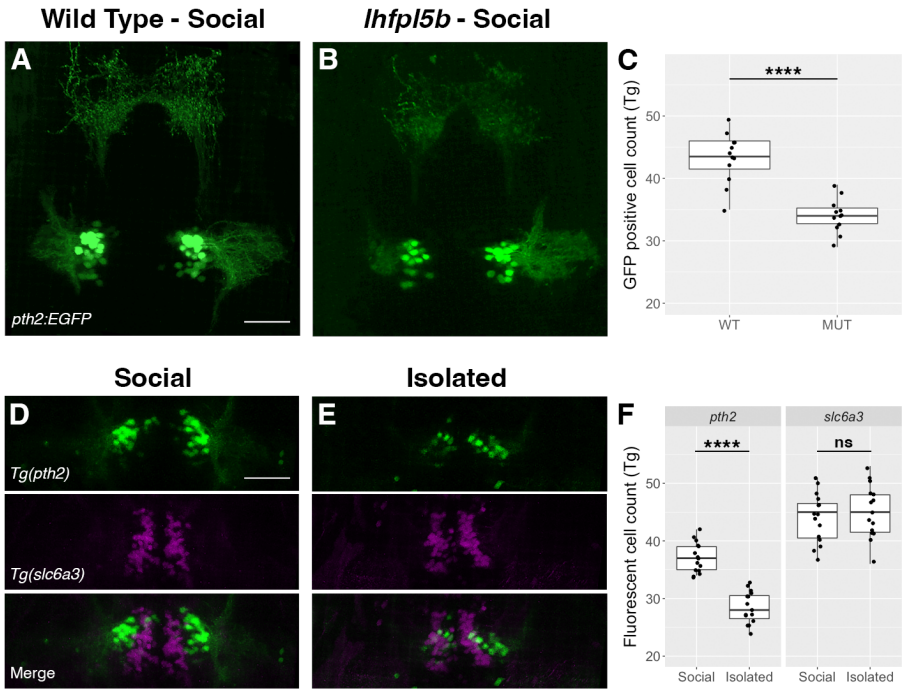

Figure 5: Effect of lateral line loss of function and social isolation on *pth2* and *slc6a3* expression using fluorescent reporters. A-B: Representative images of *Tg*(*pth2:EGFP)unb2* transgenic expression in socially-reared A) wild type and B) lateral line mutant (*lhfpl5b*^{vo35}) zebrafish. C) Boxplots of GFP-positive cell counts in wild type (WT) and *lhfpl5b* mutant (MUT) siblings. D-E: Representative images of *Tg*(*pth2:TagRFP)unb3* (false-colored green, top) and *Tg(slc6a3:EGFP)ot80* (false-colored magenta, middle) transgenes in D) socially-reared and E) isolated larvae. Merges of the two channels are shown at the bottom. F) Boxplots of *pth2* and *slc6a3* cell counts. Scale bar is 50 µm. A one-tailed Welch's t-test was used to assess significance, **** = $p < 0.0001$, ns = not significant.